Convective Stability of CO_2 Sequestration in a Porous Medium

April 10, 2020

Mahmoud H. DarAssi[1]

Department of Basic Sciences, Princess Sumaya University for Technology, Amman, Jordan.

Abstract

We considered an incompressible fluid-saturated porous layer bounded by two infinite parallel plates. Boussinesq approximation and Darcy's law are applied. The permeability is assumed to be a linear function of the depth z. The linear stability is investigated. The long wavelength expansion method is applied to conduct the weakly nonlinear stability analysis. The evolution equation is derived and analyzed. A uniformly valid periodic solution of the evolution equation is obtained by the application of Poincaré-Lindstedt method. Some numerical simulations is presented.

Key words: Stability Analysis, Long Wavelength Method, Poincaré-Lindstedt Method, Periodic Solution, Carbon Sequestration.

1 Introduction

The greenhouse effects of carbon dioxide is one of the most urgent problems that face the humaneness. The greenhouse gas emissions can be reduced through the geological carbon dioxide sequestration in deep rock formulations. Geological carbon dioxide sequestration is the process of trapping CO_2 that produced by buring fossil fuels or any other chemical or biological processes and placing it in a deep rock formulation (thousands of feet deep) for long-term storage so that it will not affect the atmosphere.

---

[1]Corresponding author. Email: m.assi@psut.edu.jo

1

26 This process comprising of three stages: Capturing, transporting, and injecting CO_2
27 into geological formulation such as gas reservoirs, unmineable coal seams, and Basalt
28 formulations [1]-[4]. The capacity of such formulations is estimated worldwide to be
29 between 675-900 Gt carbons in the gas reservoirs, between 1000-10000 Gt for Saline
30 aquifers, and for unmineable coal is between 3-200 Gt of carbon. Depends on the
31 geothermal gradient and the fluid properties CO_2 migrates and reacts with the rocks
32 formulation. Hence, many trapping mechanisms such as structure trapping, residual-
33 phase trapping, solubility trapping, and mineral trapping have been contributed to
34 retention the CO_2 sequestration for a very long period [5].
35 In the past few decades, the interest in the understanding of the convection in porous
36 media has been increased. Vast of studies have been made in several branches of engi-
37 neering and sciences[6]-[23]. Natural convection in porous media has been explored in
38 numerous articles. Horton and Rogers in 1945 and Lapwood in 1948, have studied the
39 stability analysis of the convection of a fluid in a porous medium for a horizontal fluid
40 layer problem. The critical Rayleigh number was $4\pi^2$ [6, 7]. Foster [8, 9], applied the
41 amplification theory to study a time dependent coefficients of a system of partial dif-
42 ferential equations. They determined the onset of instability in terms of critical time.
43 King et. al., use the amplification method to study the carbon dioxide sequestration
44 problem in anisotropic porous media [10, 11]. The problem of convection of carbon
45 dioxide storage in saline aquifers has been investigated by Hassanzadeh et. al. [12]-[14]
46 and Emami-Meybodi et. al. [15, 16]. A step-function base profile has been considered
47 by Wanstall and Hadji [17]. They conducted the stability analysis by performing the
48 normal modes approach. They investigated the linear and nonlinear stability analysis
49 to obtain the minimum thickness of the layer of the saturated brine that is required to
50 the fluid motion.
51 Neufeld et. al. [18], performed laboratory experiments to study the convective be-
52 havior of CO_2 brine. Their numerical simulations depicted the relation between the
53 convective flux and the Rayleigh number. To study the dissolution of CO_2 into brine,
54 Neufeld et. al. [19] used mixtures of methanol and ethylene-glycol solutions in water in
55 their laboratory experiments. Batchelor and Nitsche [20], considered the small distur-
56 bance to stationary stratified fluid. They showed numerically that the growth rate is a
57 function of the Rayleigh number, the Prandtl number, and the horizontal wavenumber
58 of the disturbance. A nonlinear stability analysis of a convection in porous layer with
59 finite conducting boundaries has been conducted by Riahi [21]. Hill and Morad [22],
60 have studied the convective stability in an anisotropic porous medium. They consid-
61 ered a water-saturated porous layer bounded by two horizontal parallel plates. The
62 Darcy equation with variable permeability is used to govern the fluid motion.
63 Vo and Hadji [23], investigated the linear and weakly nonlinear stability analyses of
64 the convection induced by sequestration of CO_2 in a perfectly impervious geological
65 formulation. They considered a horizontal layer of brine saturated porous medium

confined between two horizontal planes that are impermeable to mass flow. They used the classical normal modes to investigate the linear stability. The weakly nonlinear stability is conducted by applying the long wavelength asymptotic expansion method that is valid for small Damköhler numbers. They determined that the Rayleigh number and its corresponding wavenumber are independent of the depth of the formulation. Vo and Hadji [23], described the model that mimics the Rayleigh-Taylor instability to study the carbon sequestration. They considered the heavy carbon-saturated layer ,$(Z_0\ 1]$ on the top of light free-carbon layer, $[0\ Z_0)$. This situation leads to very thin unstable stratified layer at $z = Z_0$ a cross which buoyancy diffuses. The stratified basic profile is defined as step function and the reference carbon concentration in porous media is defined by

$$C_{ref}(z) = \begin{cases} 0 & 0 < z < Z_0 \\ \dfrac{z - Z_0}{1 - Z_0} & Z_0 < z < 1. \end{cases}$$

The basic temperature profile is defined by $T_B = T_1 + (T_2 - T_1)\mathcal{H}(z - Z_0)$, where T_1 and T_2 are temperature values at the lower region and the upper region, respectively and $\mathcal{H}$ is the Heaviside function.

In this paper, we considered the same model that has been proposed by Hill and Morad [22]. Where the instability is quantified in term of long time evolution with the Dirichlet and Neumann boundary conditions at the top and lower walls respectively.

This paper is organized as follows: In section (2), a full description of the problem is presented and the problem is governed by a mathematical model. Moreover, the basic profile of the concentration is derived. In section (3), the steady-state linear stability is conducted. The weakly nonlinear stability is investigated by the application of the long wavelength exapansion method in section (4). In section (5), The Poincaré-Lindstedt method is used to obtain a uniformly valid periodic solution. Numerical simulations are intoduced and the results are concluded in section (6).

2   Mathematical Formulation

In this section we considered the mathematical model that has been discussed by Hill and Morad [22], Wanstall and Hadji [17], and Vo and Hadji [23]. That is we considered an incompressible fluid-saturated porous layer bounded by two infinite horizontal parallel plates. We assumed that the Boussinesq approximation and the Darcy's law are applied and the fluid motion is governed by the Darcy equation. Therefore, the nondimensionalized governing system of equations comprised of Darcy's equation, continuity equation, the conservation of carbon dioxide equation, and the equation of solute balance is given by

$$\nabla \cdot \mathbf{u} = 0 \tag{1a}$$

$$\frac{1}{\mathcal{F}(z)}\,\mathbf{u} = \nabla\,p - c\,\mathbf{k} \tag{1b}$$

$$\frac{\partial c}{\partial \hat{t}} + \mathbf{u}\cdot\nabla\,c + \left(\frac{dM(z)}{dz}\right)w = \frac{\xi}{R}\,\nabla_H^2\,c + \frac{1}{R}\left(\frac{\partial^2 c}{\partial z^2} - Da\,c\right) \tag{1c}$$

$$\rho = \rho_0\left[1 + \gamma_c\,(c - C_0)\right] \tag{1d}$$

where $M(z)$ is the basic profile of concentration, p is the pressure, $\mathbf{k}$ is the vertical unit vector, ρ_0 is the reference density, $\xi = \dfrac{\kappa_h}{\kappa_v}$ is the ratio of the horizontal and vertical solutal difusion, $\mathcal{F}(z)$ is the z-dependent dimensionless permeability, $Da = \dfrac{\beta\,H^2}{\psi_p\,\kappa_v}$ is the Damökhler number, β is the reaction rate and the control parameter, namely, the Rayleigh-Darcy number $R = \dfrac{\gamma_c\,g\,H\,K_0\,C_0}{\phi_p\,\nu\,\kappa_\nu}$, where γ_c is the solutal expansion, g is the gravitational constant, H is the distance between the two plates, K_0 is the reference permeability value, C_0 is the reference concentration of CO_2, ϕ_p is the porosity, ν is the kinematic viscosity, and κ_ν is the vertical CO_2 diffusion coefficient. Subject to the following boundary conditions:

$$\mathbf{u} = \mathbf{0}, \quad \text{at} \quad z = 0,\ z = 1$$

and

$$\frac{\partial c}{\partial z} = 0, \quad \text{at} \quad z = 0,\ z = 1$$

For more details about this model please refer to [22], [17] and [23]. Figure (1), describes the problem with its boundary conditions.

The step function base state is modeled by the partial differential equation

$$\frac{\partial C_B}{\partial \hat{t}} = \frac{1}{R}\left(\frac{\partial^2 C_B}{\partial z^2} - Da\,C_B\right), \quad 0 \le z \le 1, \quad t > 0 \tag{2}$$

subject to the boundary conditions

$$\frac{\partial C_B}{\partial z} = 0 \quad \text{at} \quad z = 0, \quad z = 1$$

and initial condition

$$C_B(z,0) = \begin{cases} 0 & 0 \le z < Z_0 \\ 1 & Z_0 \le z \le 1. \end{cases}$$

The solution of equation (2) is given by

$$C_B(z,\hat{t}) = 1 - Z_0 - 2\sum_{n=1}^{\infty} \frac{\sin(n\pi\,Z_0)}{n\pi}\,\cos(n\pi\,z)\exp\left(-\frac{Da + n^2\,\pi^2}{R}\,\hat{t}\right) \tag{3}$$
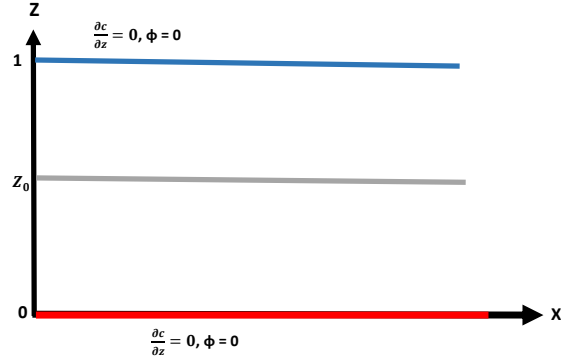
4

Figure 1: An incompressible fluid-saturated porous layer bounded by two infinite horizontal parallel plates.
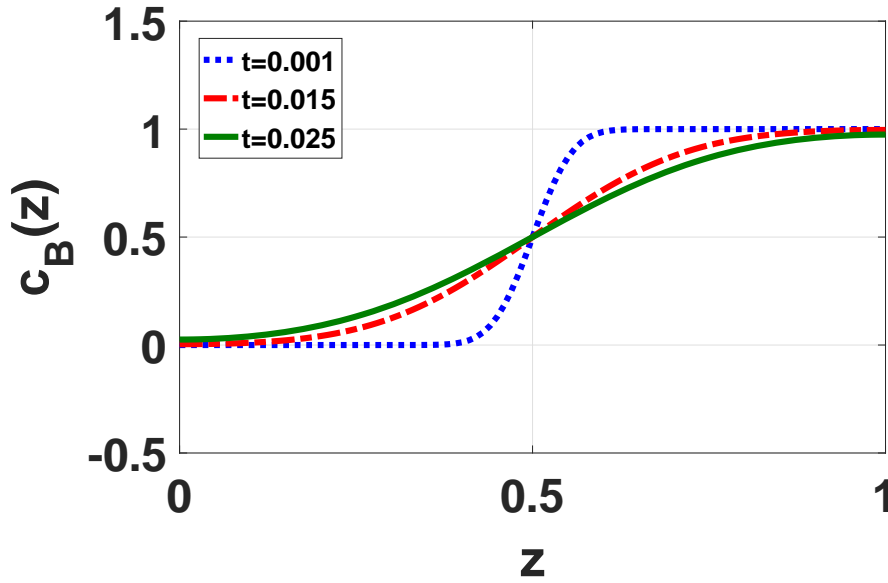

Figure 2: The plot of the concentration profile $c_B(z)$ as a function of the depth of the fluid layer z and $t = 0.001$ (dotted line), $t = 0.015$ (dashed line) and $t = 0.025$ (solid line).

Figure (2) bellow shows the plot of the concentration basic profile as a function of z for some values of t.

Following [17], the basic concentration profile consists of a light layer $0 < z < Z_0$ under a heavier one, $Z_0 < z < 1$ which can be described by the Heaviside function i.e. $M(z) = \mathcal{H}(z - Z_0)$. Upon subtracting the basic state profiles, introducing the poloidal representation for the velocity field $\mathbf{u} = \nabla \times (\nabla \times \phi \, \mathbf{k})$, and considering the vertical component of the velocity we removed the pressure term and the system of equations (1a)-(1d) reduced to

$$\mathcal{F}(z)\nabla^2\phi - \mathcal{F}'(z)\frac{d\phi}{dz} = -\mathcal{F}^2(z)\,c \tag{4a}$$

$$c_{\hat{t}} + (\nabla_H\phi_z)\cdot(\nabla_H c) - \nabla_H^2\,\phi\,c_z = -\nabla_H^2\,\phi\,\delta(z-Z_0) + \frac{\xi}{R}\nabla_H^2 c + \frac{1}{R}\left(\frac{\partial^2 c}{\partial z^2} - Da\,c\right) \tag{4b}$$

where ϕ is the poloidal representation for the divergence velocity field, $\delta(z - Z_0)$ is the Dirac delta function, c is the deviation of the concentration in volume fraction from the diffusive state, R is Rayleigh-Decay number, and $\nabla_H = (\partial/\partial x, \partial/\partial y)$. Subject to the following Boundary conditions

$$\phi = 0 \text{ at } z = 0, 1, \text{ and } \frac{\partial c}{\partial z} = 0 \text{ at } z = 0,\; z = 1 \tag{5}$$

Upon introducing the transformation $\Phi = R\,\phi$ and $\dfrac{\partial}{\partial t} = R\dfrac{\partial}{\partial \hat{t}}$ the equations (4a) and (4b) reduced to

$$\mathcal{F}(z)\nabla^2\Phi - \mathcal{F}'(z)\frac{d\Phi}{dz} = -R\,\mathcal{F}^2(z)\,c \tag{6a}$$

$$c_t + (\nabla_H\Phi_z)\cdot(\nabla_H c) - \nabla_H^2\,\Phi\,c_z = -\nabla_H^2\,\Phi\,\delta(z-Z_0) + \xi\nabla_H^2 c + \left(\frac{\partial^2 c}{\partial z^2} - Da\,c\right) \tag{6b}$$

Subject to the following Boundary conditions

$$\Phi = 0 \text{ at } z = 0, 1, \text{ and } \frac{\partial c}{\partial z} = 0 \text{ at } z = 0,\; z = 1 \tag{7}$$

To investigate the linear and weakly nonlinear stability we will assume $\xi = 1$, the convection effect dominates over the reaction effect i.e. $Da = 0$ and $\mathcal{F}(z) = 1 + \lambda z$, $|\lambda| < 1$, see [22]. Hence, equations (6a) and (6b) become

$$(1 + \lambda z)\nabla^2\Phi - \lambda\frac{d\Phi}{dz} = -R\,(1+\lambda z)^2\,c \tag{8a}$$

$$c_t + (\nabla_H\Phi_z)\cdot(\nabla_H c) - \nabla_H^2\,\Phi\,c_z = -\nabla_H^2\,\Phi\,\delta(z-Z_0) + \nabla_H^2 c + \frac{\partial^2 c}{\partial z^2} \tag{8b}$$

Subject to the following Boundary conditions

$$\Phi = 0 \text{ at } z = 0, 1, \text{ and } \frac{\partial c}{\partial z} = 0 \text{ at } z = 0,\; z = 1 \tag{9}$$

3 Steady-state linear stability analysis

Following the standard procedure used in [24], we obtained the following linearized system of equations governing the convective perturbations

$$(1 + \lambda z)\nabla^2\phi - \lambda\frac{d\Phi}{dz} = -(1 + \lambda z)^2 R c \tag{10a}$$

$$\nabla^2 c = -\nabla_H^2 \phi\, \delta(z - Z_0) \tag{10b}$$

Subject to the following Boundary conditions

$$\Phi = 0 \text{ at } z = 0, 1, \text{ and } \frac{\partial c}{\partial z} = 0 \text{ at } z = 0, \ z = 1 \tag{11}$$

To investigate the linear stability we will introduce the normal modes

$$\Phi = e^{i\alpha\cdot\mathbf{x}}W(z)(z), \quad c = e^{i\alpha\cdot\mathbf{x}}S(z). \tag{12}$$

where $\mathbf{x} = (x, y)$ and $|\alpha| = \alpha$, we obtained

$$(1 + \lambda z)(D^2 W(z) - \alpha^2 W(z)) = -(1 + \lambda z)^2 R S(z) \tag{13a}$$

$$(D^2 - \alpha^2)\, S(z) = \alpha^2\, W(z)\, \delta(z - Z_0) \tag{13b}$$

where $D = \frac{d}{dz}$. The corresponding Dirichlet and Neumann boundary conditions are $W = 0$ at $z = 0, 1$, $DS = 0$ at $z = 0, 1$.

Expand W, S and R in terms the small wave number α and keep λ of order 1. $W = W_0 + \alpha^2 W_2 + \cdots$, $S = S_0 + \alpha^2 S_2 + \cdots$ and $R = R_0 + \alpha^2 R_2$. The $O(1)$ problem is given by

$$D\left[\frac{1}{1 + \lambda z}\, DW_0\right] = -R_0\, S_0 \tag{14a}$$

$$D^2 S_0 = 0 \tag{14b}$$

Subject to the boundary conditions $W_0(0) = W_0(1) = 0$ and $DS_0(0) = DS_0(1) = 0$. The solution of the equations (14a) and (14b) is given by

$$S_0 = 1$$

$$W_0 = -\frac{R_0\, G}{6}\left[(3z^2 + 2\lambda z^3) - L_1(2z + \lambda z^2)\right]$$

Where $L_1 = ((3/2) + \lambda)(1 - \lambda/2)$.

Proceeding to the next order $O(\alpha^2)$, the equation of the concentration becomes

$$D^2 S_2 - S_0 = W_0\, \delta(z - Z_0) \tag{15}$$

7

which has a unique solution if and only if the follwing condition is satisfied:

$$\int_0^1 S_0^* \left[S_0 + W_0 \, \delta(z - Z_0) \right] dz = 0$$

where S_0^* is the solution of the adjoint problem of equation (14b), namely $D^2 S_0^* = 0$ with corresponding boundary conditions $DS_0^*(0) = DS_0^*(1) = 0$ to get $S_0^* = 1$. Upon applyong the Fredholm alternative at $O(\alpha^2)$ we obtain that the critical Rayleigh-Darcy number

$$R_0 = \frac{6}{L_1(2Z_0 + \lambda Z_0^2) - (3Z_0^2 + 2\lambda Z_0^3)}$$

As $\lambda \to 0$ the critical Raleigh-Dracy number becomes $R_0 = \dfrac{2}{Z_0 - Z_0^2}$ which is consistent with what had been obtained in [17]. Figure (3) depicts that plot of the critical Rayleigh-Dracy number R_0 is decresded as the values of λ have increased in the right figure and the left figure shows that the minimum value of the critical Rayleigh-Dracy number R_0 is at $Z_0 = 0.5$ and it goes to infinity as Z_0 approaches 0 or 1.
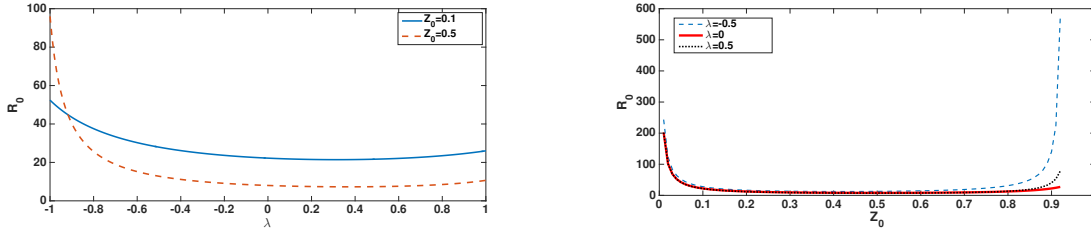

Figure 3: (Right) Plot of the critical Rayleigh-Dracy number R_0 as a function of λ for $Z_0 = 0.1$ (solid line) and $Z_0 = 0.5$ (dashed line). Plot of the critical Rayleigh-Dracy number R_0 as a function of Z_0 for $\lambda = 0$ (solid line), $\lambda = -0.5$ (dashed line) and $\lambda = 0.5$ (dotted line). (Left)

4   Weakly nonlinear stability

In this section we will investigate the weakly nonlinear stability by deriving the evolution equation. Following the long wavelength analysis procedure used in [25] and [26] we introduce the small parameter $\epsilon \ll 1$ and we scale $X = \epsilon x$, $Z = z$, $\tau = \epsilon^4 t$ and keep λ of $O(1)$ quantity in equations (8a) and (8b). Moreover, we expand

$$\Phi = \Phi_0 + \epsilon^2 \Phi_2 + \cdots, \qquad c = c_0 + \epsilon^2 c_2 + \epsilon^4 c_4 + \cdots$$

and $R = R_0 + \epsilon^2 \widehat{\mu}^2$. The solution of leading order proplem that is described by

$$(1 + \lambda Z) D^2 \Phi_0 - \lambda D \Phi_0 = -(1 + \lambda Z)^2 R_0 \, c_0 \tag{16a}$$

8

$$D^2 c_0 = 0 \tag{16b}$$

with boundary conditions $\Phi_0(0) = \Phi_0(1) = 0$ and $Dc_0(0) = Dc_0(1) = 0$ is given by

$$\Phi_0 = -\frac{R_0\,h}{6}\left[(3Z^2 + 2\lambda Z^3) - L_1\,(2\,Z + \lambda Z^2)\right]$$

$$c_0 = h(X,\tau)$$

167 where $L_1 = (1.5 + \lambda)(1 - \lambda/2)$.

168 Proceeding to the next order, the $O(\epsilon^2)$ problem is described by

$$D^2\Phi_2 - \lambda D\Phi_2 + (\Phi_0)_{XX} = -(1 + \lambda Z)[R_0\,c_2 + \widehat{\mu}^2\,c_0] \tag{18a}$$

169

$$(D\Phi_0)_X\,(c_0)_X = -(\Phi_0)_{XX}\,\delta(Z - Z_0) + D^2 c_2 + (c_0)_{XX} \tag{18b}$$

170 Application of the solvability condition on equation (18b), yields

$$R_0 = \frac{6 + 3\lambda}{(3 + 2\lambda)(Z_0 + (\lambda/2)Z_0^2) - (3Z_0^2 + 2\lambda Z_0^3)(1 + \lambda/2)} \tag{19}$$

171 As $\lambda \to 0$ the critical Raleigh-Dracy number becomes $R_0 = \dfrac{2}{Z_0 - Z_0^2}$ which is consistent

172 with what had been obtained in [17]. Proceeding to solve $O(\epsilon^2)$ problem and because

173 of the appearance of the $\delta(Z - Z_0)$ term we will divide the problem in two cases and

174 equation (18b) will be divided into two equations

The light layer when $0 < Z < Z_0$: $D^2 c_2^- = -R_0\,(c_0)_X^2\,(Z + \lambda Z^2) - (c_0)_{XX}$ (20a)

175

The heavy layer when $0 < Z < Z_0$: $D^2 c_2^+ = -R_0\,(c_0)_X^2\,(Z + \lambda Z^2) - (c_0)_{XX}$ (20b)

with boundary conditions $Dc_2^-(0) = 0$ and $Dc_2^+(1) = 0$. Thus, the solutions of equations (20a) and (20b) are

$$c_2^- = -\frac{R_0\,(h_X)^2}{36}\left[6Z^3 + 3\lambda Z^4 - L_1(3Z^2 + \lambda\,Z^3)\right] - \frac{h_{XX}}{2}\,Z^2 + A^-$$

$$c_2^+ = -\frac{R_0\,(h_X)^2}{36}\left[6Z^3 + 3\lambda Z^4 - L_1(3Z^2 + \lambda\,Z^3)\right] - \frac{h_{XX}}{2}(Z^2 - 2\,Z) + A^+$$

176 where $A^- = Z_0\,h_{XX} + A^+$ and

177

$A^+ = \dfrac{R_0\,(h_X)^2}{720}\left[(30 + 12\lambda) - 5\,L_1(4 + \lambda)\right] - \dfrac{h_{XX}}{6}(2 + 3\,Z_0^2)$. Similarly, the solution of equation (18a) is given by

$$\Phi_2^- = -\frac{R_0\,h_{XX}}{10080}\left[92\lambda^3\,Z^7 + (182 - 35\,L_1)\,\lambda^2\,Z^6 - (588\lambda + 98\lambda^2\,L_1)\,Z^5 - (840 + 140\lambda\,L_1)\,Z^4\right.$$

$$+L_1 - ((1680\,Z_0^2 - 3360\,Z_0 + 1120)\,\lambda - 280\,L_1)\,Z^3 - (2520\,Z_0^2 - 5040\,Z_0 + 1680)\,Z^2]$$

$$+\frac{R_0^2\,(h_X)^2}{30240}\left[72\lambda^2\,Z^7 + (294\lambda - 35\,L_1)\,Z^6 + (252 - 210\,\lambda\,L_1)\,Z^5 - 210\,L_1\,Z^4 - (168\,\lambda^2) + 420\,\lambda\right.$$

$$\left. -70\,L_1(4\lambda + \lambda^2))\,Z^3 - (252\lambda + 630 - 105\,L_1\,(4 + \lambda))\,Z^2\right] - \frac{\widehat{\mu}^2\,h}{6}\,(2\lambda\,Z^3 + 3\,Z^2) + \frac{B^-}{2}(\lambda\,Z^2 + 2\,Z)$$

$$\Phi_2^+ = -\frac{R_0\,h_{XX}}{10080}\left[92\lambda^3\,Z^7 + (182 - 35\,L_1)\,\lambda^2\,Z^6 - (588\lambda + 98\lambda^2\,L_1)\,Z^5 + (1260\lambda - 3360 - 70\lambda\,L_1)\,Z^4\right.$$

$$\left. -((1680\,Z_0^2 + 1120)\,\lambda - 1680 - 280\,L_1)\,Z^3 - (2520\,Z_0^2 + 1680)\,Z^2\right]$$

$$+\frac{R_0^2\,(h_X)^2}{30240}\left[72\lambda^2\,Z^7 + (294\lambda - 35\,L_1)\,Z^6 + (252 - 210\,\lambda\,L_1)\,Z^5 - 210\,L_1\,Z^4 - (168\,\lambda^2) + 420\,\lambda\right.$$

$$\left. -70\,L_1(4\lambda + \lambda^2))\,Z^3 - (252\lambda + 630 - 105\,L_1\,(4 + \lambda))\,Z^2\right] - \frac{\widehat{\mu}^2\,h}{6}\,(2\lambda\,Z^3 + 3\,Z^2) + \frac{B^+}{2}(\lambda\,Z^2 + 2\,Z) + A^{++}$$

where

$$B^+ = \frac{R_0\,h_{XX}}{15120\,(2 + \lambda)}\left[(288\lambda^3 - 546\lambda^2 - (1260\,Z_0^4 + 5040\,Z_0^2 + 1344)\lambda + 5040\,Z_0^3 + 7560\,Z_0^2 + 2520)\right.$$

$$\left. -L_1(105\lambda^3 + 294\lambda^2 - 420\lambda - 840)\right]$$

$$+\frac{R_0^2\,(h_X)^2}{15120\,(2 + \lambda)}\left[(96\lambda^2 + 378\lambda - 378 - L_1\,(35\lambda^2 + 175\lambda + 210)\right] + \frac{L1\,\widehat{\mu}^2\,h}{3}.$$

$$B^- = \frac{Z_0^2\,R_0\,h_{XX}}{2} + B^+$$

$$A^{++} = \frac{R_0\,h_{XX}}{10080}\left[96\lambda^3 + 182\lambda^2 - (1680\,Z_0^2 + 448)\lambda + (840 - 1260\lambda) - 2520\,Z_0^2 - 840\right.$$

$$\left. -L_1(35\lambda^3 + 98\lambda^2 - 140\lambda - 280)\right]$$

$$+\frac{R_0^2\,(h_X)^2}{30240}\left[(96\lambda^2 + 378\lambda + 378 - L_1\,(35\lambda^2 + 175\lambda + 210)\right]$$

$$+\frac{\widehat{\mu}^2\,h}{6}(2\lambda + 3) - \frac{B^+}{2}(2 + \lambda).$$

178 Proceeding to the next order $O(\epsilon^4)$, we have

$$D^2 c_4 = h_\tau + h_X\,(D\Phi_2)_X - (\Phi_0)_{XX}\,Dc_2 + (D\Phi_0)_X\,(c_2)_X + (\Phi_2)_{XX}\,\delta(Z - Z_0) - (c_2)_{XX} \quad (22)$$

179 with boundary conditions $Dc_4(0) = Dc_4(1) = 0$. Integrating equation (22) with respect
180 to Z from $Z = 0$ to $Z = 1$, yields the sought evolution equation

$$h_\tau = -\mathcal{A}\,h_{XXXX} - \widehat{\mu}^2\mathcal{B}\,h_{XX} + \mathcal{C}\,(h_X)_{XX}^2 + \mathcal{E}\,h_X^2\,h_{XX} \quad (23)$$

10

Where

$$\mathcal{A} = -\frac{R_0\left(Z_0 - Z_0^2\right)}{10080\left(2+\lambda\right)}\left\{[35(Z_0^4 + Z_0^3 + Z_0^2 + Z_0)\,L_1 - 96(Z_0^5 + Z_0^4 + Z_0^3 + Z_0^2 + Z_0)]\lambda^4+\right.$$

$$[(70Z_0^4 + 168Z_0^3 + 168Z_0^2 + 168Z_0 + 70)\,L_1 - (192Z_0^5 + 374Z_0^4 + 374Z_0^3 + 374Z_0^2 + 374Z_0 + 192)]\lambda^3$$

$$+[(196Z_0^3 + 56Z_0^2 + 56Z_0 + 196)\,L_1 - (784Z_0^4 - 1484Z_0^2 - 84Z_0 + 364)]\lambda^2$$

$$\left.-[280(Z_0^2 + 2Z_0 + 1)\,L_1 - 56(36Z_0^3 + 21Z_0^2 + Z_0 + 16)]\lambda - 560(Z_0 + 1)\,L_1 - 1680(2Z_0^2 - Z_0 + 1)\right\}$$

$$\mathcal{B} = \frac{1}{3}\left(Z_0 - Z_0^2\right)\left(\lambda Z_0 + L_1\right)$$

$$\mathcal{C} = \frac{R_0^2\left(Z_0 - Z_0^2\right)}{30240\left(2+\lambda\right)}\left\{[(72Z_0^5 + 72Z_0^4 + 72Z_0^3 + 72Z_0^2 - 96Z_0) - 35(Z_0^4 + Z_0^3 + Z_0^2 + Z_0)\,L_1]\lambda^3+\right.$$

$$[(144Z_0^5 + 438Z_0^4 + 438Z_0^3 + 438Z_0^2 - 318Z_0 - 192) - (70Z_0^4 + 280Z_0^3 + 280Z_0^2 - 140Z_0 - 70)\,L_1]\lambda^2+$$

$$[(588Z_0^4 + 840Z_0^3 + 840Z_0^2 - 756) - (420Z_0^3 + 630Z_0^2 + 70Z_0 - 350)\,L_1]\lambda$$

$$\left.+504Z_0^3 + 504Z_0^2 + 504Z_0 - 756 - 420(Z_0^2 + Z_0 - 1)\,L_1\right\}$$

$$\mathcal{E} = \frac{R_0^2}{30240}\left[96\lambda^2 + 504\lambda + 756 - (84\lambda^2 + 476\lambda + 870)\,L_1 + (21\lambda^2 + 140\lambda + 280)\,L_1^2\right]$$

The evolution equation 23 is of parabolic type which is wellposed whenever the coefficient of the fourth derivative, $-\mathcal{A}$, is negative. Figure 4 shows that $-\mathcal{A}$ is negative for all valueas of λ and Z_0.
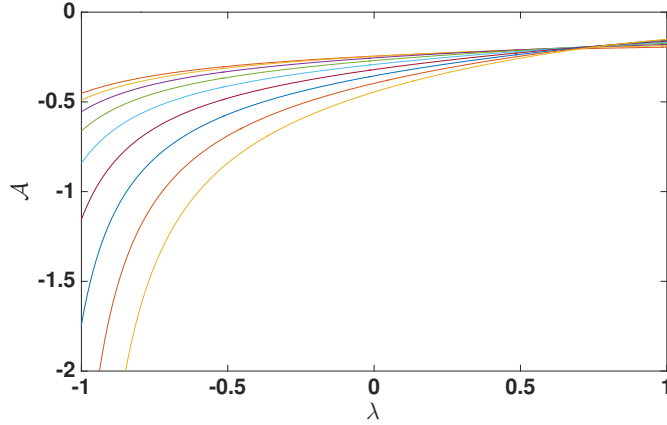

Figure 4: The plot of $\mathcal{A}$ as a function of λ, where $|\lambda| < 1$ and $0 \le Z_0 \le 1$.

5 Uniformly Valid Periodic Solution

Upon using the general procedure of Biot number [27], the term $-\widehat{\gamma}\,h$ will be added to equation (23) to obtain

$$h_\tau = -\mathcal{A}\,h_{XXXX} - \widehat{\mu}^2\mathcal{B}\,h_{XX} - \widehat{\gamma}\,h + \mathcal{C}\,(h_X)^2_{XX} + \mathcal{E}\,h_X^2\,h_{XX} \qquad (24)$$

11

Upon Introducing the following scaleas and transformations $h = a\,f$, $\quad \xi = b\,X$, $\quad \tau = e\,\widehat{\tau}$, $\quad \gamma = a\,\widehat{\gamma}$ and $e = 1/a$ we have

$$f_\tau = -f_{\xi\xi\xi\xi} - 2\mu^2\,f_{\xi\xi} - \gamma\,f + \Gamma\,(f_\xi)^2_{\xi\xi} + (f_\xi)^2\,f_{\xi\xi} \tag{25}$$

where

$$a = \sqrt{\frac{\mathcal{A}}{\mathcal{E}}}, \quad b = \left(\frac{1}{\mathcal{A}}\sqrt{\frac{\mathcal{E}}{\mathcal{A}}}\right)^{1/4}, \quad \Gamma = \frac{\mathcal{C}}{\sqrt{\mathcal{A}\,\mathcal{E}}} \quad \text{and} \quad \mu^2 = \frac{\widehat{\mu}^2\,a\,b^2}{2}$$

. To invetigate the stability of the static solution of equation (25) we consider the linear part

$$f_\tau = -f_{\xi\xi\xi\xi} - 2\mu^2\,f_{\xi\xi} - \gamma\,f \tag{26}$$

Introducing the normal modes $f(\xi,\tau) = e^{\sigma\tau + i\theta\,\xi}$, the following dispersion relation is obtained

$$\sigma = -(\theta^2 - \mu^2) + \mu^4 - \gamma \tag{27}$$

Therefore, the trivial static solution, $f = 0$, is unstable when $\gamma < \mu^4$. Upon introducing the small parameter $\epsilon \ll 1$, the weakly nonlinear stability of the evolution equation can be investigated. To conduct the perturbation analysis around the linear solution, we expand

$$\gamma = \mu^4 - \epsilon\,\gamma_1 - \epsilon^2\,\gamma_2, \quad \tau = \epsilon^2\,\eta$$

and

$$f = \epsilon\,f_1 + \epsilon^2\,f_2 + \epsilon^3\,f_3 + \cdots$$

The $O(\epsilon)$ problem of equation (25) is described by

$$(f_1)_{\xi\xi\xi\xi} + 2\mu^2\,(f_1)_{\xi\xi} + \gamma\,f_1 = 0 \tag{28}$$

Whose period solution on the interval $\left(\dfrac{-\pi}{\mu}, \dfrac{\pi}{\mu}\right)$ is $f_1 = \cos(\mu\,\xi)$. Because of the secular terms that are expected due to the linear part and the nonlinear terms, we will apply the Poincaré-Lindstedt method [28] to obtain a uniformly valid periodic solution. Substituting $\nu = \omega\,\xi$ and expanding $\omega = 1 + \epsilon\,\omega_1 + \epsilon^2\,\omega_2 + \cdots$ in equation (25) to obtain

$$\omega^4\,f_{\nu\nu\nu\nu} + 2\mu^2\,\omega^2\,f_{\nu\nu} + \gamma\,f = \omega^4[\Gamma\,(f_\nu)^2_{\nu\nu} + (f_\nu)^2\,f_{\nu\nu}] \tag{29}$$

Define the operator $\mathcal{L}(f) = f_{\nu\nu\nu\nu} + 2\mu^2\,f_{\nu\nu} + \mu^4\,f$. The leading order problem is described by

$$\mathcal{L}(f_1) = (f_1)_{\nu\nu\nu\nu} + 2\mu^2\,(f_1)_{\nu\nu} + \mu^4\,f_1 = 0 \tag{30}$$

Whose solution is $f_1 = \cos(\mu\,\nu)$. The $O(\epsilon^2)$ problem is described by

$$\mathcal{L}(f_2) = \gamma_1\,\cos(\mu\nu) + \mu^4\,\cos(2\mu\nu) \tag{31}$$

12

To remove the mixed-secular terms we set $\gamma_1 = 0$, that is there is no subcritical instability. Thus, the solution of $\mathscr{L}(f_2) = \mu^4 \cos(2\mu\nu)$ is $f_2 = \frac{1}{9} \cos(2\mu\nu)$. Proceeding to the next order, the $O(\epsilon^3)$ problem is described by

$$\mathscr{L}(f_3) = \left[\gamma_2 - 4\,\omega_1^2\,\mu^4 - \frac{\Gamma\,\mu^4}{4} - \frac{5\mu^4}{9} \right] \cos(\mu\nu) - \frac{20\omega_1\,\mu^4}{9} \cos(2\mu\nu) + \left[\frac{\Gamma\mu^4}{4} + \frac{5\mu^4}{9} \right] \cos(3\mu\nu) \tag{32}$$

To remove the secular term, we set $\gamma_2 - 4\,\omega_1^2\,\mu^4 - \dfrac{\Gamma\,\mu^4}{4} - \dfrac{5\mu^4}{9} = 0$ and then we solve for ω_1 to get

$$\omega_1 = \pm\sqrt{\frac{\gamma_2}{4\mu^4} - \frac{\Gamma}{16} - \frac{5}{36}}$$

Therefore, the solution of equation (32) is given by

$$f_3 = -\frac{5\omega_1}{36} \cos(2\mu\nu) + \frac{9\Gamma + 20}{2916} \cos(3\mu\nu) \tag{33}$$

Thus, a uniformly valid steady state of equation (25) is given by

$$f = \epsilon\,\cos((1+\epsilon\omega_1)\xi\mu) + \epsilon^2\,\frac{1}{9}\,\cos(2(1+\epsilon\omega_1)\xi\mu) + \epsilon^3\,\left[-\frac{5\omega_1}{36} \cos(2(1+\epsilon\omega_1)\xi\mu) + \frac{9\Gamma + 20}{2916} \cos(3(1+\epsilon\omega_1)\xi\mu) \right] \tag{34}$$

Figure (5) shows the the plot of the uniformly valid periodic solution of equation (25) as a function of ξ for $\gamma_2 = 10$ and $\mu = 0.7$.
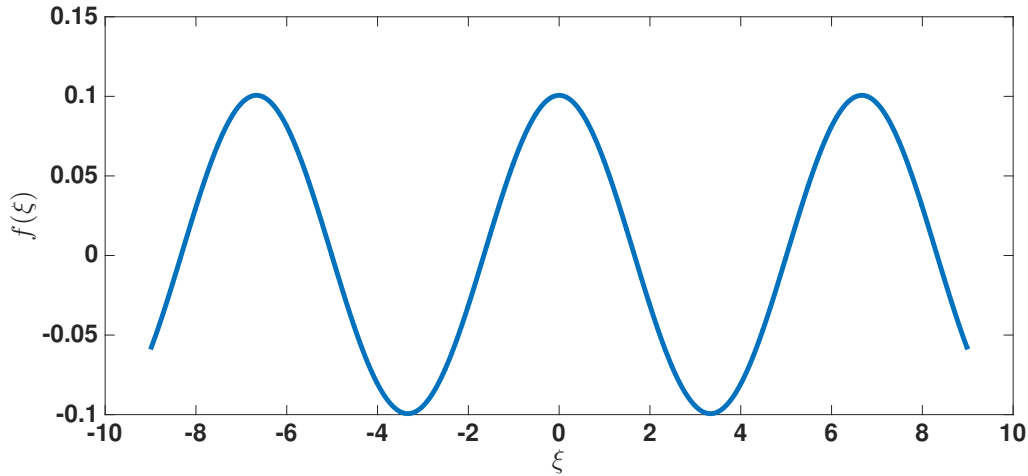

Figure 5: A plot of the periodic solution of equation (25) as a function of ξ with $\gamma_2 = 10$ and $\mu = 0.7$.

13

6 Conclusion

In this paper, we studied the mathematical model that was proposed by Hill and Morad [22]. That is we considered an incompressible fluid-saturated porous layer bounded by two infinite parallel plates. Boussinesq approximation and Darcy's law are applied. The permeability is assumed to be a linear function of the depth z, namely, $\mathcal{F}(z) = 1 + \lambda z$. The base state of the model is consisting of a light free-carbon layer, $[0, Z_0)$ at the bottom and a havier carbon-saturated layer, $(Z_0, 1]$ at the top, figures (1) and (2) illustrate the problem. Steady-state linear stability analysis is conducted and the critical Rayleigh -Darcy number is obtained, namely, $R_0 = \dfrac{6}{L_1(2Z_0 + \lambda Z_0^2) - (3z_)^2 + 2\lambda Z_0^3)}$. If we let $\lambda \to 0$, then the critical Rayleigh-Darcy numbedr becomes $R_0 = \dfrac{2}{Z_0 - Z_0^2}$, which is consistent with the value obtained in [17]. The relation between the critical Rayleigh-Darcy number and the permeability coefficient λ is depicted in figure (3).

The long wavelength expansion method is applied to derive the evolution equation (23). Figure (6) shows the velocity, Φ_0 as a function of the depth Z for different values of the permeability coefficient λ.
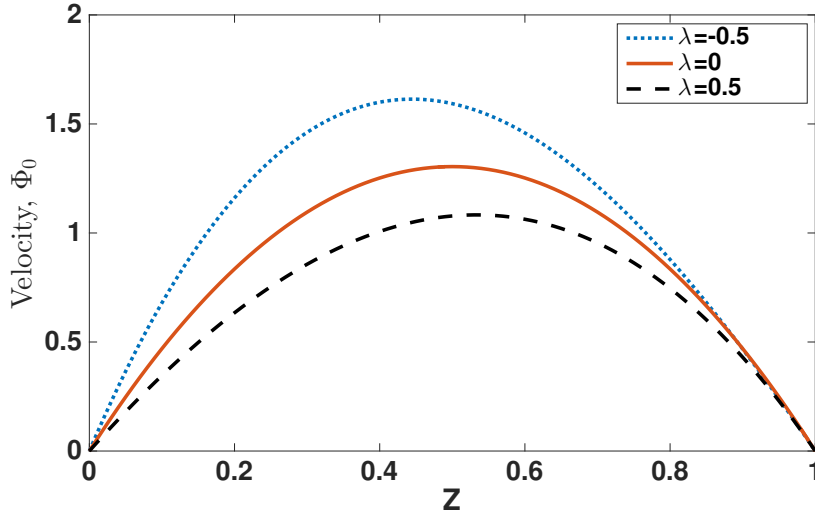

Figure 6: The plot of the velocity Φ_0 as a function of the depth Z with $\lambda = -0.5$ (dotted line), $\lambda = 0$ (solid line) and $\lambda = 0.5$ (dashed line).

Moreover, the dispersion equation is obtained and the relation between the growth rate, biot number and the weve number is depicted in figure (7) and a uniformly valid periodic solution is obtained by the application of the Poincaré-Lindstedt method and the plot of the solution is shown in figure (5).
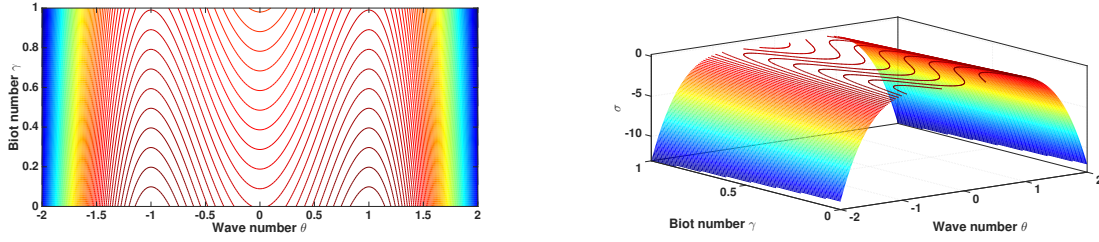
14

Figure 7: The 2D plot of the growth rate σ as a function of the wave number θ and the biot number γ (left figure) and the 3D plot (right figure) with $\mu = 0.7$.

References

[1] Sedjo R. and Sohngen B. Carbon Sequestration in Forests and Soils. *Annual Reviews* **2012**, *4*, 127-144, https://doi.org/10.1146/annurev-resource-083110-115941.

[2] Bachu S. Sequestration of CO_2 in geological media in response to climate change: road map for site selection using the transform of the geological space into the CO_2 phase space . *Energy Convers Mgmt* **2002**, *43*, 87-102, DOI. 10.1016/S0196-8904(01)00009-7

[3] Bachu S. Sequestration of CO2 in geological media: criteria and approach for site selection in response to climate change. *Energy Convers Mgmt* **2000**, *41*, 953-970, DOI.10.1016/S0196-8904(99)00149-1

[4] U.S. Department of Eenergy. Carbon Sequestration Key R&D Programs and Initiatives. *https://www.energy.gov/fe/science-innovation/carbon-capture-and-storage-research.*

[5] International Panel on Climate Change. Carbon Dioxide Capture and Storage. *Cambridge University Press* **2005**.

[6] Horton C. W. and Rogers F. T. Convection currents in porous media. *J. Appl. Phys.* **1945**, *16*, 367-369, DOI. 10.1063/1.1707601

[7] Lapwood E. R. Convection of a fluid in porous medium. *Proc. Cambridge Phil. Soc.* **1948**, *44*, 508-521, DOI. 10.1017/S030500410002452X

[8] Foster T. Onset of convection in a layer of fluid cooled from above. *Phys. Fluids* **1965**, *8*, 1770-1774. DOI. 0.1063/1.1761108

[9] Foster T. Onset of manifest convection in a layer of fluid with time-dependent surface temperture. *Phys. Fluids* **1969**, *12*, 2482-2487. DOI. 10.1063/1.1692384

[10] Ennis-King J. P. and Paterson L. Role of convective mixing in the long-term storage of carbon dioxide in deep saline formulations. *Soc. Pet. Eng.* **2005**, *10*, 349-356.

[11] Ennis-King J. P., Preston I. and Paterson L. Onset of convection in anisotropic porous media subject to a rapid change in boundary conditions. *Phys. Fluids* **2005**, *17*, (084107) 1-15. DOI. 10.1063/1.2033911

[12] Hassanzadeh H., Poolladi-Darvish M., and Keith D. W. Modelling of Convective Mixing in CO_2 Storage. *J. Can. Petrol. Technol.* **2005**, *44*, 43-51. DOI. 10.2118/2004-151

[13] Hassanzadeh H, Poolladi-Darvish M., and Keith D. W. Stability of a fluid in a horizontal saturated porous layer: effect of non-linear concentration profile, initial, and boundary conditions. *Transp Porous Med.* **2006**, *65*, 193-211. DOI. 10.1007/s11242-005-6088-1

[14] Hassanzadeh H., Poolladi-Darvish M., and Keith D. W. Scaling Behavior of Convective Mixing, with Application to Geological Storage of CO_2. *AIChEJ* **2007**, *53*, 1121-1131. DOI. 10.1002/aic.11157

[15] Emami-Meybodi H., Hassanzadeha H., Greenb C.P., and Ennis-King J. Convective dissolution of CO_2 in saline aquifers: Progress in modelingand experiments. *International Journal of Greenhouse Gas Control* **2015**, *40*, 238-266. DOI. 10.1016/j.ijggc.2015.04.003

[16] Emami-Meybodi H., Hassanzadeha H., and Ennis-King J. CO_2 dissolution in the presence of background flow of deep saline aquifers. *Water Resources Research* **2015**, *51*, 2595-2615. DOI. 10.1002/2014WR016659

[17] Wanstall C. T. and Hadji L. A step function density profile model for the convective stability of CO_2 geological sequestration. *J Eng. Math.* **2018**, *108*, 53-71. DOI. 10.1007/s10665-017-9907-9

[18] Neufeld J., Hesse M., Riaz A., Hallworth M., Techelepi H., and Huppert H. Convective dissolution of carbon dioxide in saline aquifers. *Geophsical Research Letters* **2010**, *37*, L22404. DOI. 10.1029/2010GL044728

[19] Neufeld J., Vella D., and Huppert H. The effect of a fissure on storage in a porous medium. *J. Fluid Mech.* **2009**, *639*, 239-259. DOI. 10.1017/S0022112009991030

[20] Batchelor G. and Nitsche J. Instability of stationary unbounded stratified fluid. *J. Fluid Mech.* **1991**, *227*, 357-391. DOI. 10.1017/S0022112091000150

[21] Riahi N. Nonlinear convection in a porous layer with finite conducting boundaries. *J. Fluid Mech.* **1983**, *129*, 153-171. DOI. 10.1017/S0022112083000701

[22] Hill A. and Morad, M. Convective stability of carbon sequestration in anisotropic porous media.*Proceedings of the Royal Society A* **2014**, *470* 2170. DOI. 10.1098/rspa.2014.0373

[23] Vo L. and Hadji L. Weakly nonlinear convection induced by the sequestration of CO2 in a perfectly impervious geological formation. *Physics of Fluids* **2017**, *29* 127101. DOI.10.1063/1.4998253

[24] Drazin P.G. and Reid W.H. *Hydrodynamic Stability.* Cambridge University Press: Cambridge, UK, 2004.

[25] Busse F.H. and Riahi N. Nonlinear thermal convection with poorly conducting boundaries. *J. Fluid Mech.* **1980**, *96*, 243-256.

[26] Chapman C.J. and Proctor M.R.E. Nonlinear Rayleigh-Bénrad convection between poorly conducting boundaries. *J. Fluid Mech.* **1980**, *101*, 759-782.

[27] Proctor M.R.E. Planform selection by finite-amplitude thermal convection between poorly conducting slabs. *J. Fluid Mech.* **1981**, *113*, 469-485.

[28] Nayfeh A.H. Introduction to perturbation techniques. **2004**, *139*. Wiley, New Yourk.